NASA TECHNICAL NOTE

WIND-TUNNEL INVESTIGATION OF
THE STATIC AERODYNAMIC CHARACTERISTICS
OF A MULTILOBE GLIDING PARACHUTE

by George M. Ware and Charles E. Libbey

Langley Research Center
Langley Station, Hampton, Va.

WIND-TUNNEL INVESTIGATION OF

THE STATIC AERODYNAMIC CHARACTERISTICS

OF A MULTILOBE GLIDING PARACHUTE

By George M. Ware and Charles E. Libbey

Langley Research Center
Langley Station, Hampton, Va.

NATIONAL AERONAUTICS AND SPACE ADMINISTRATION

WIND-TUNNEL INVESTIGATION OF
THE STATIC AERODYNAMIC CHARACTERISTICS
OF A MULTILOBE GLIDING PARACHUTE

By George M. Ware and Charles E. Libbey
Langley Research Center

SUMMARY

An investigation has been conducted in the Langley full-scale tunnel to determine the performance and static stability and control characteristics of a five-lobe gliding parachute. The model was completely void of any rigid structural members and utilized only the tension forces produced by aerodynamic loading to maintain the shape of the canopy. The configuration consisted of a five-lobe canopy, roughly rectangular in inflated planform with an airfoil-type leading edge. The tests were made over an angle-of-attack range from the lowest angle attained before wing collapse, which was about 22.5^O to 90°, which corresponded approximately to the vertical-descent condition.

The results indicate that maximum lift occurred at an angle of attack of about 25°. The model was longitudinally stable and could be trimmed at angles of attack from the minimum angle of the tests to 30°. In the angle-of-attack range from 30° to 75°, the model had no stable trim conditions but was stable and could be trimmed at angles of attack from 75° to 90°. The stable trim angle-of-attack ranges gave values of lift-drag ratio of 2.2 to about 1.5 in the lower angle range and values near 0 in the higher angle range. The model was directionally stable and had positive effective dihedral at the lower angles of attack, but was directionally unstable and had negative effective dihedral over much of the range of angles of attack above 30°. Similarly, the model had satisfactory static lateral-control characteristics at angles of attack up to about 45°; however, because of a reversal in the direction of the yawing moment with control deflection, the model had unsatisfactory control characteristics at the higher angles of attack.

INTRODUCTION

There is, at the present time, an increasing interest in controllable gliding parachutes as a means of space-vehicle recovery and cargo delivery, and there are a number of different types of gliding parachutes being developed to meet the demand for such a system. In order to evaluate the performance, stability and control, and deployment

characteristics of this type of configuration, the Langley Research Center is presently evaluating several parachute-like devices with gliding capability by means of wind-tunnel and flight tests.

One configuration in the gliding-parachute category which has received considerable attention consists of a multiple-lobe canopy, roughly rectangular in inflated planform with span greater than chord and having an airfoil-type leading edge. The air loads are carried into the suspension lines through catenaries which are shaped to maintain a low chordwise camber in the canopy. The particular model used in the present investigation was based on a five-lobe canopy design. This model was also one of the subjects of tests reported in reference 1. The present investigation consisted of static wind-tunnel force tests to determine the basic lift and drag characteristics and the longitudinal and lateral stability and control characteristics of the model over an angle-of-attack range from the lowest value attainable without wing collapse to that corresponding to the vertical-descent condition and over a sideslip range from -10° to 10°. The tests were conducted at a dynamic pressure of about 1.0 pound per square foot (47.9 N/m^2).

SYMBOLS

The data are referred to the stability system of axes. The origin of the axes was located to correspond to a center-of-gravity position at the confluence point of the suspension lines. The coefficients are based on the laid-out-flat canopy area of 95.5 square feet (8.87 square meters), the center-line chord length of 4.5 feet (1.37 meters), and the wing span of 15 feet (4.57 meters). Measurements used in this investigation were taken in the U.S. Customary System of Units. Equivalent values are indicated parenthetically herein in the International System of Units (SI). Details of this system, together with conversion factors, can be obtained in reference 2.

b span of inflated wing, feet (meters)

C_D drag coefficient, $\dfrac{D}{qS}$

C_L lift coefficient, $\dfrac{L}{qS}$

C_l rolling-moment coefficient, $\dfrac{\text{Rolling moment}}{qSb}$

$C_{l_\beta} = \dfrac{\partial C_l}{\partial \beta}$, per degree

C_m pitching-moment coefficient, $\dfrac{\text{Pitching moment}}{qSc}$

C_n yawing-moment coefficient, $\dfrac{\text{Yawing moment}}{qSb}$

$C_{n_\beta} = \dfrac{\partial C_n}{\partial \beta}$, per degree

C_Y lateral-force coefficient, $\dfrac{\text{Lateral force}}{qS}$

$C_{Y_\beta} = \dfrac{\partial C_Y}{\partial \beta}$, per degree

c center-line chord length, feet   (meters)

D drag, pounds   (newtons)

F_A axial force, pounds   (newtons)

F_R resultant force, pounds   (newtons)

L lift, pounds   (newtons)

L/D lift-drag ratio

M moment about the upper balance, foot-pounds   (meter-newtons)

q free-stream dynamic pressure, pounds per square foot   (newtons per square meter)

S wing area, square feet   (square meters)

W payload weight, pounds   (newtons)

W_C canopy and lines weight, pounds   (newtons)

x_1 distance between suspension-line confluence point and moment center of upper strain-gage balance of support system, feet   (meters)

x_2 distance between suspension-line confluence point and center of gravity of canopy and suspension lines, feet   (meters)

α angle of attack (angle between relative wind and wing-chord plane perpendicular to center post), degrees; center post defines a line from suspension-line confluence point to midpoint of center-line chord of canopy

β angle of sideslip, degrees

γ angle between horizon and relative wind, degrees

Δl change in length of suspension line being used as a control, feet (meters); negative value indicates decreasing line length

Subscripts:

L   left

R   right

APPARATUS AND TESTS

Model

A plan-view drawing of the model in a laid-out-flat condition and a front view of the inflated configuration are presented in figure 1. A sketch and a photograph of the model mounted for force testing in the Langley full-scale tunnel are presented in figures 2 and 3, respectively. Some of the more important items of the test setup are labeled in figure 2. The fabric used to form the canopy of the model was 1.6-ounce-per-square-yard (0.0542-kg/m^2) rip-stop nylon cloth with an acrylic coating which reduced the porosity to less than 10 cubic feet per minute (0.0047 m^3/sec) at a pressure of 10 inches (25.4 cm) of water. The air loads were carried into the 12 suspension lines through catenary curtains which also acted as ribs to aid in maintaining a predetermined chordwise camber in the canopy. The model was equipped with two control lines, as shown in figure 1. These lines were shortened together as a pitch control or individually as a lateral-directional control.

Model Support

The model-support system used in this investigation was the same apparatus that was used in the tests of reference 3, with modifications made to accommodate the present model. The model was mounted on a long center post that was pivoted in the middle to permit changes in angle of attack. The reference angle of attack of the wing was defined as the angle between the relative wind and the wing-chord plane perpendicular to the

4

center post. The suspension lines of the model were attached to a bar at the lower end of the center post, which spread the lines laterally by about 18 inches (45.7 cm). The canopy was restrained by three short spikes (one on the center post and two on the cross arm) which were inserted through small clearance holes in the fabric at three chord mid-points. The spikes were instrumented with strain-gage balances to measure the axial force and moment at the canopy. With this mounting system, the model was restrained in roll, pitch, and yaw in such a way that fabric and line stretch were virtually unaffected. The entire wing-support system was mounted on a turntable which was attached to the full-scale-tunnel force-measuring scales. Changes in angle of sideslip were accomplished by rotating the turntable.

Test Procedure

The investigation was conducted in the Langley full-scale tunnel, a complete description of which is given in reference 4. The lift and drag characteristics of the model were determined from measurements obtained from the tunnel scale-balance system. The pitching-moment characteristics, however, were obtained from the strain gages attached to the spikes at the model canopy. The strain-gage measurements were used to eliminate the possible errors in pitching moment involved with small inaccuracies in force measurements when forces were transferred over the long moment-arm distances in the tunnel measurement system. A sketch showing how the force and moment measured by the strain-gage balances and the model-weight component were used to compute the pitching-moment coefficient is presented in figure 4. The lateral tests were made by using the tunnel force-measuring system inasmuch as the model was not instrumented with strain gages to read lateral forces and moments.

Test Conditions

The data were obtained over the angle-of-attack range from about 22.5^o to 90° and at angles of sideslip from -10° to 10°. The tests were conducted at a dynamic pressure of 1.0 pound per square foot (47.9 N/m^2). The test Reynolds number based on the model chord length of 4.5 feet (1.37 meters) was 0.86×10^6. The data are presented with no wind-tunnel corrections applied.

Comparison of Wind-Tunnel and Flight Conditions

There are certain differences between the model under the wind-tunnel test conditions and the model in free flight which might have some effect on the test results and should be noted. It is necessary to restrain the model during the static wind-tunnel tests, but the method of restraint used in the present investigation, as pointed out previously, is felt to allow the model to assume the shape dictated by aerodynamic loading, with little

apparent distortion in the canopy. The shape of the all-flexible model, however, is also affected by its canopy weight, and the weight vector is in a different direction under static force-test conditions in a horizontal wind tunnel than in free-gliding flight. Sketches showing the longitudinal forces for the free-flight and wind-tunnel conditions are presented in figures 5(a) and 5(b), respectively. In free-gliding flight, the weight vector of the canopy passes approximately through the suspension-line confluence point, which in this case has been assumed to be the center of gravity. In a horizontal wind tunnel, however, the canopy-weight vector passes far behind the confluence point of the lines and contributes a nose-up pitching moment which is not present during free flight. An indication of the magnitude of this moment may be seen in figure 5(c). Although both the longitudinal and lateral data presented in this paper have been corrected for the canopy-weight tare, the effect of the direction of the weight vector of individual elements of the canopy and suspension lines on the shape and therefore the aerodynamic characteristics of the canopy has not been determined. This effect may be significant at low angles of attack, where the leading edge of the wing is lightly loaded. At these low angles, the small weight effects of the relatively light canopy suspension lines might cause the leading edge of the wing to collapse at a slightly higher angle of attack in the wind tunnel than in free flight.

RESULTS AND DISCUSSION

Longitudinal Characteristics

The lift, drag, and longitudinal stability characteristics of the model are presented in figure 6. Data are presented for three individual tests made under the same conditions, and the results indicate good repeatability over the entire test angle-of-attack range. The minimum angle of attack reached during these tests was about 22.5°; below this angle, the wing would not remain inflated. The maximum value of the lift coefficient of about 0.97 occurred at an angle of attack slightly greater than the minimum angle — about 25°. The lift coefficient then decreased with increasing angle of attack. The maximum value of the lift-drag ratio was 2.25 and occurred at the lowest angle of attack attainable of 22.5°. The pitching-moment data show that the model was stable over the test angle-of-attack range and had decreasing stability above 30°.

The longitudinal control characteristics of the model are presented in figure 7. With the control lines in the fully extended position, the model was trimmed at the minimum test angle of attack. Shortening the control lines was effective in trimming the model to higher angles of attack. Although the maximum control-line change of the investigation, $\dfrac{\Delta l_{L \text{ and } R}}{b} = -0.033$, moved the trim point only to $\alpha = 26^\circ$, the trend of the data indicates that with greater control deflections, the model may have stable trim points up

to an angle of attack of about 30°. Above 30°, the model with control deflections became longitudinally unstable. The trim characteristics indicate a possible lift-drag-ratio modulation from 2.2 to about 1.5 in the stable low angle-of-attack range. With control deflections, the model also had stable trim points with accompanying lift-drag ratios near 0 in the angle-of-attack range from about 75° to 90°, which corresponds to vertical descent.

It should be pointed out, however, that during preliminary gliding tests of a similar configuration, attempts to trim the model from the low to the high angle-of-attack range resulted in asymmetric wing stall which caused the model to go into a tight spiraling flight with an accompanying high rate of descent. In some cases of model stall, the wing became visibly deformed with a pronounced sweepback.

Lateral Characteristics

Because of the restraint imposed by the model-support spikes which passed through the canopy at three spanwise positions (see fig. 2), the model could be held at various angles of sideslip. Whether or not the model could attain these angles in free flight and what deformation might occur are unknown. The data are therefore only gross or qualitative indications of lateral stability. The model remained relatively steady on the center post at an angle of sideslip of 0° over the entire angle-of-attack range, but the configuration became unsteady as the angle of sideslip was increased. This motion might be described as a torsional oscillation about the center-post axis which caused some deformation of the wing tips. The oscillations were particularly noticeable when the model was sideslipped at angles of attack above 40°. This occurrence, however, does not indicate that the wing would behave in this manner at angles of sideslip in free flight. The oscillation was very likely associated with the restraint provided by the mounting system.

The lateral characteristics are presented in figure 8 as the variation of the static lateral coefficients of the model with angle of sideslip for angles of attack from 22.5° to 90°. As may be seen, the curves are relatively linear at the lower angles of attack ($\alpha = 22.5^\circ$ to 40°) but show larger irregularities at the higher angles of attack. These data are summarized in figure 9 in the form of the variation of the stability derivatives C_{Y_β}, C_{n_β}, and C_{l_β} with angle of attack. The values of the stability derivatives were obtained from the slopes of the curves through $\beta = 0^\circ$. Because of the irregularities of the data, especially at the higher angles of attack, the stability derivatives are only generally indicative of the characteristics of the model. As may be seen, the model had positive values of directional stability $\left(+C_{n_\beta}\right)$ and positive effective dihedral $\left(-C_{l_\beta}\right)$ at angles of attack from the minimum angle of the tests to 30°, where it also had longitudinal stability and could be trimmed. At higher angles of attack, the lateral-directional stability fluctuated considerably. It is interesting to note that in the angle-of-attack range from 40° to 50°, the model was directionally unstable and had negative effective dihedral.

These unstable characteristics are a result of the change in sign of the lateral derivative C_{Y_β} since this parameter multiplied by its moment arm contributes significantly to directional-stability and effective-dihedral characteristics with respect to the low center-of-gravity position.

The effect of changes in length of the control lines for lateral control is presented in figure 10. Since the neutral control setting was obtained with the control lines in the fully extended position, lateral control was accomplished by shortening only one control line. From the data of figure 10, it may be seen that although there were asymmetries in the forces and moments resulting from right and left control-line changes, deflection of either wing tip produced about the same trend. The average control effectiveness obtained by taking the difference between the right and left control data of this figure and dividing by 2 is presented in figure 11. These data indicate that at angles of attack up to about 45°, the deflected wing tip, acting as a drag device, produced yawing and rolling moments which would tend to result in a coordinated turn in the direction of the lowered tip. At the higher angles of attack, however, there was a change in the sign of the yawing moment, and the lateral-control characteristics became unsatisfactory.

CONCLUSIONS

The results of the full-scale-tunnel investigation of the performance and static stability and control characteristics of a multilobe gliding parachute may be summarized as follows:

1. The model was longitudinally stable and could be trimmed at angles of attack from about 22.5° to 30°. The minimum angle of attack reached during the investigation was 22.5°; below this angle, the wing would not remain inflated. Maximum lift occurred at an angle of attack of 25°. In the angle-of-attack range from about 30° to 75°, the model had no stable trim conditions but was stable and could be trimmed at higher angles of attack.

2. The trim angle-of-attack ranges gave values of lift-drag ratio of 2.2 to about 1.5 at the lower angles of attack and about 0 at angles near 90°.

3. The model was directionally stable and had positive effective dihedral at the lower angles of attack but was directionally unstable and had negative effective dihedral over much of the angle-of-attack range above 30°.

8

4. The model had satisfactory static lateral-control characteristics at angles of attack up to about 45° but, because of a reversal in the direction of the yawing moment with control deflection, control characteristics at the higher angles of attack were unsatisfactory.

Langley Research Center,
    National Aeronautics and Space Administration,
        Langley Station, Hampton, Va., April 23, 1968,
            124-07-03-06-23.

REFERENCES

1. Weiberg, James A.; and Mort, Kenneth W.: Wind-Tunnel Tests of a Series of Parachutes Designed for Controllable Gliding Flight. NASA TN D-3960, 1967.

2. Mechtly, E. A.: The International System of Units — Physical Constants and Conversion Factors. NASA SP-7012, 1964.

3. Libbey, Charles E.; Ware, George M.; and Naeseth, Rodger L.: Wind-Tunnel Investigation of the Static Aerodynamic Characteristics of an 18-Foot (5.49-Meter) All-Flexible Parawing. NASA TN D-3856, 1967.

4. DeFrance, Smith J.: The N.A.C.A. Full-Scale Wind Tunnel. NACA Rep. 459, 1933.

Laid—out—flat plan view

Control-line attachment points

Leading edge

Leading edge

Inflated span

Rib A

Rib B   Rib B

Catenary
curtains

Control line   Control line

Rib A   Rib B

Reference area,	95.5 ft^2	(8.87 m^2)
Inflated span,	15.0 ft	(4.57 m)
Inflated maximum chord,	4.5 ft	(1.37 m)

Front view

0   1.0
Scale, meters

0   40
Scale, inches
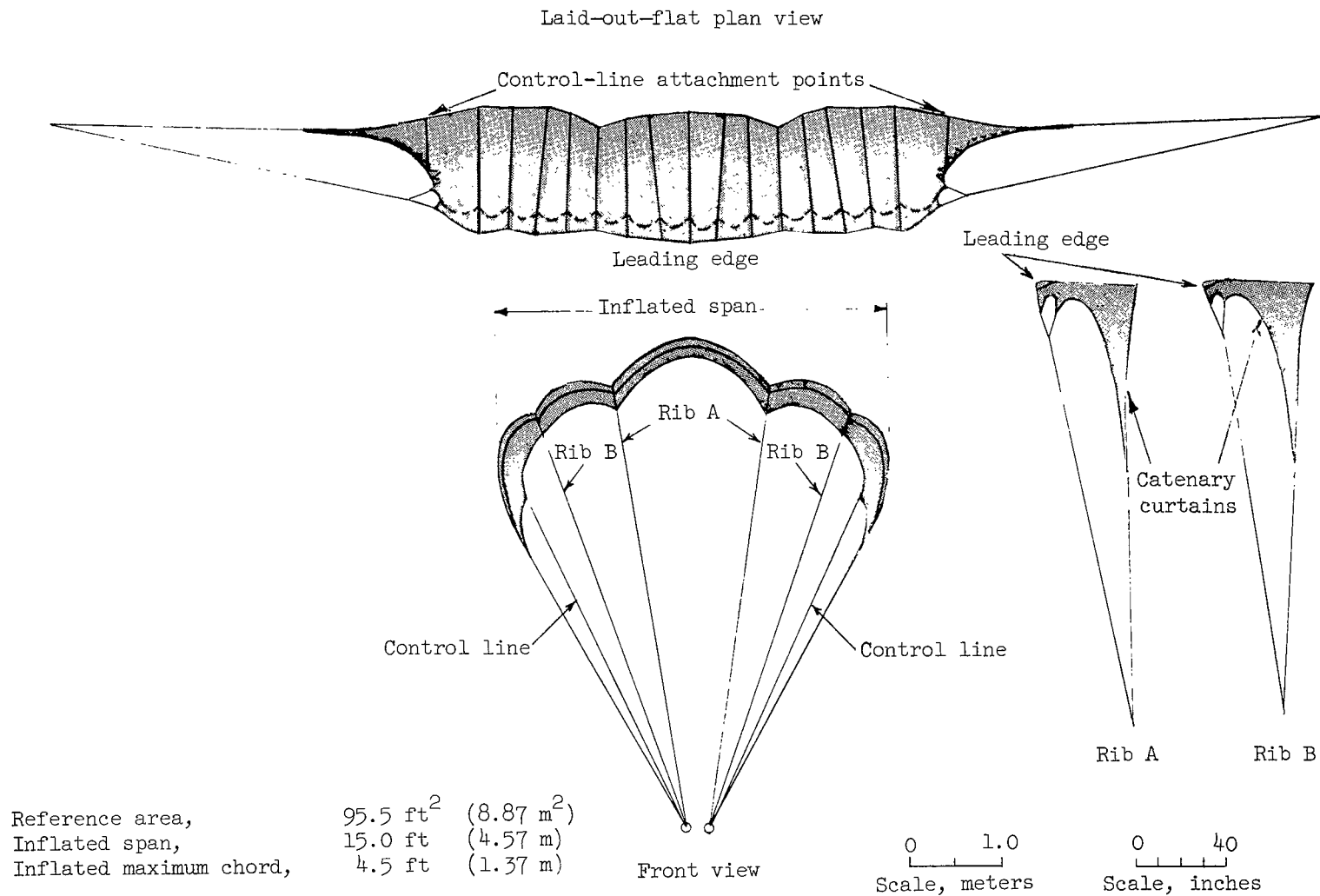
Figure 1.- Sketches of model used in the investigation.

Strain-gage balances

Angle-of-attack actuator

Center post

Support strut

Turntable attached to tunnel
force-measuring system
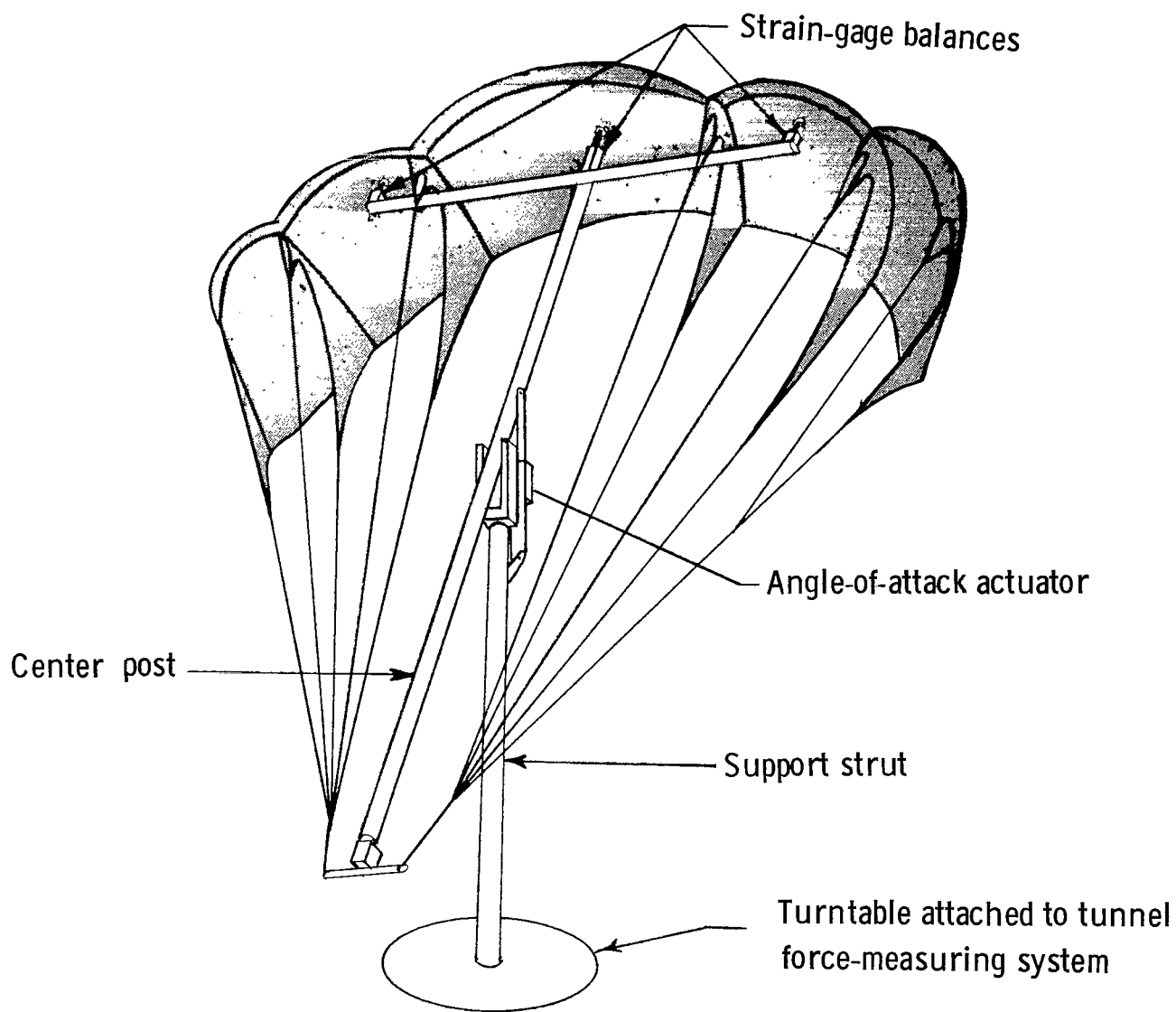
Figure 2.- Drawing showing center-post force-test apparatus in the Langley full-scale tunnel.

11
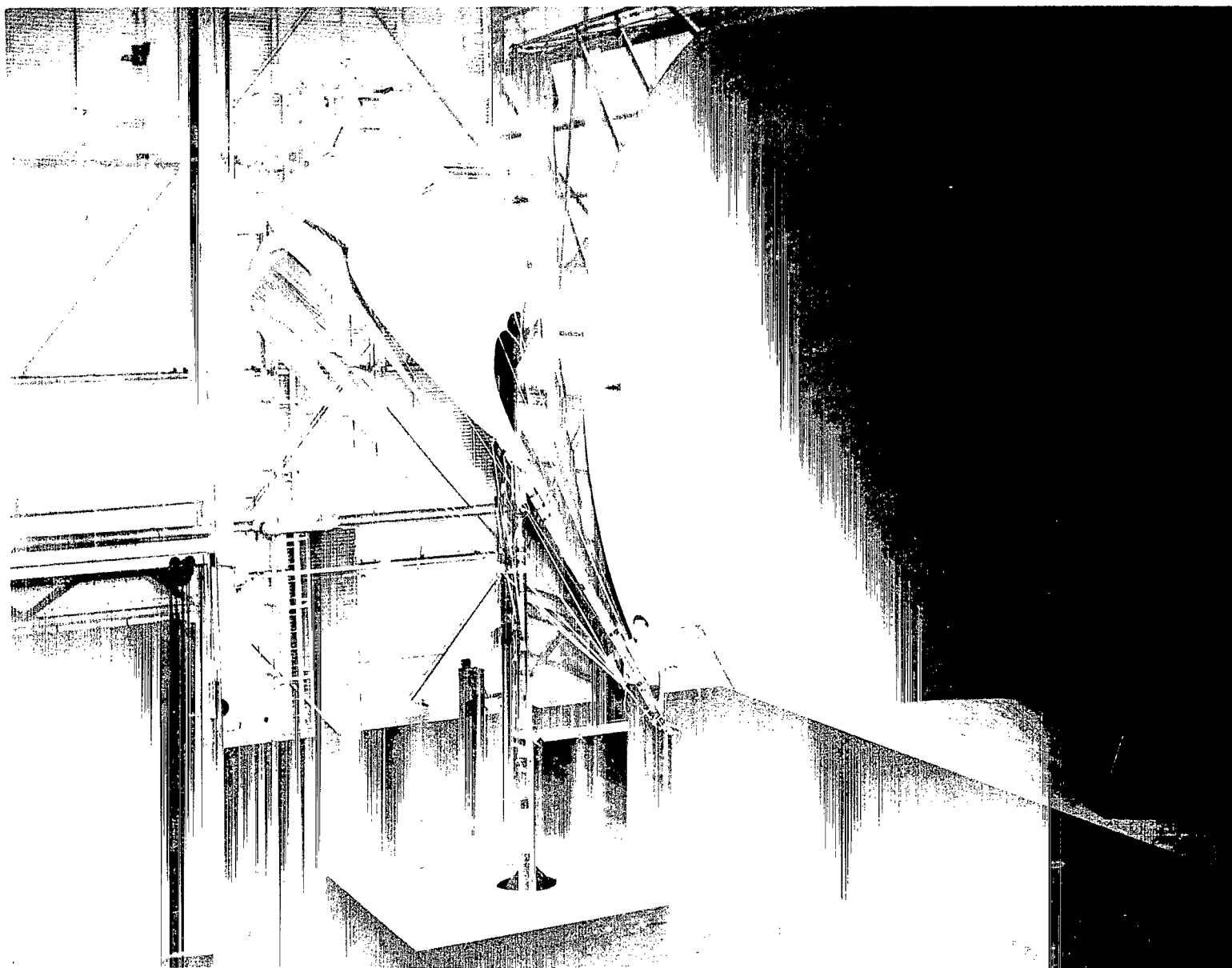
Figure 3.- Photograph of the model mounted in the Langley full-scale tunnel.
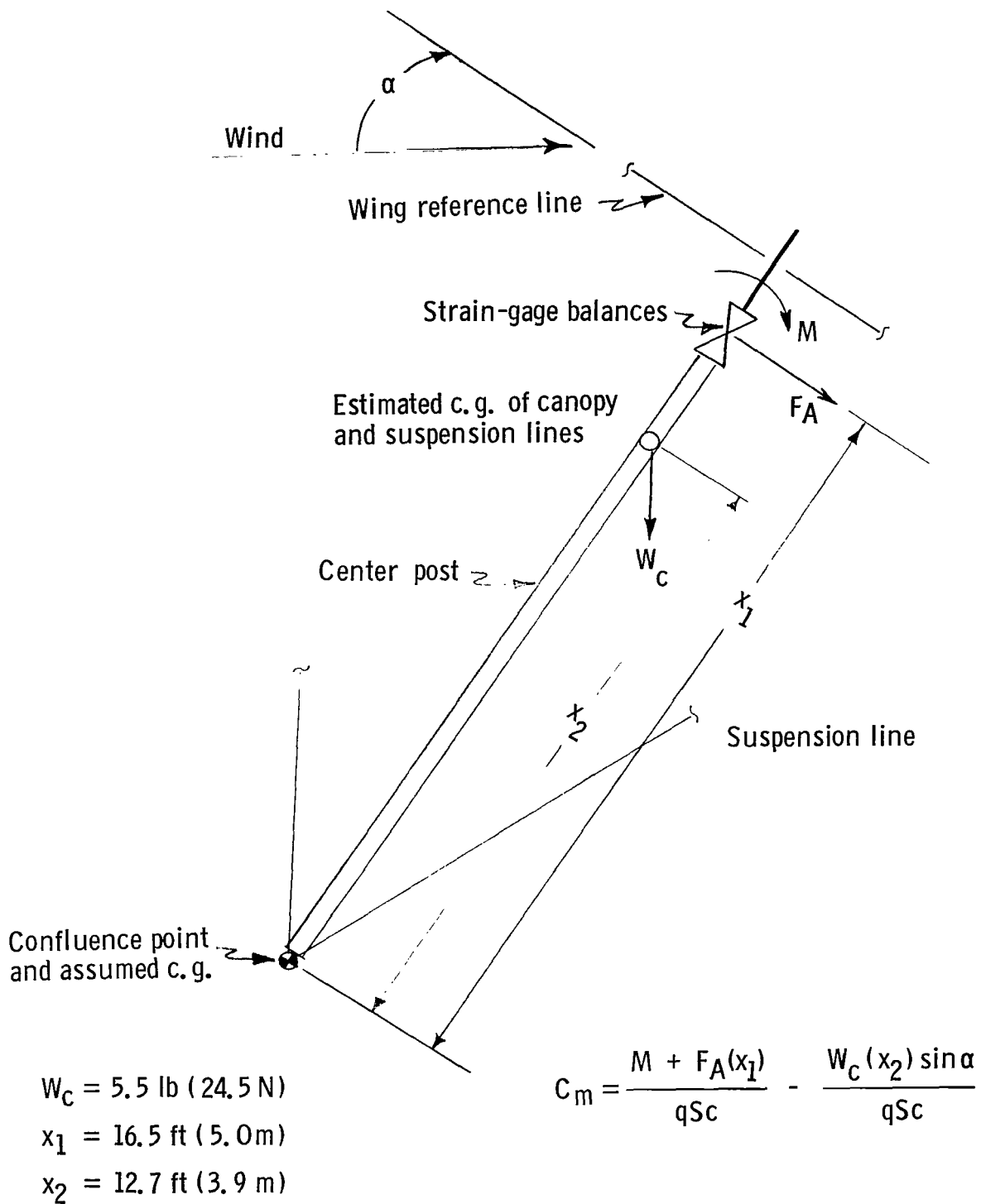
Figure 4.- Sketch showing how pitching-moment coefficient was computed.

$$W_c = 5.5 \text{ lb } (24.5 \text{ N})$$

$$x_1 = 16.5 \text{ ft } (5.0\text{m})$$

$$x_2 = 12.7 \text{ ft } (3.9 \text{ m})$$

$$C_m = \frac{M + F_A(x_1)}{qSc} - \frac{W_c(x_2)\sin\alpha}{qSc}$$
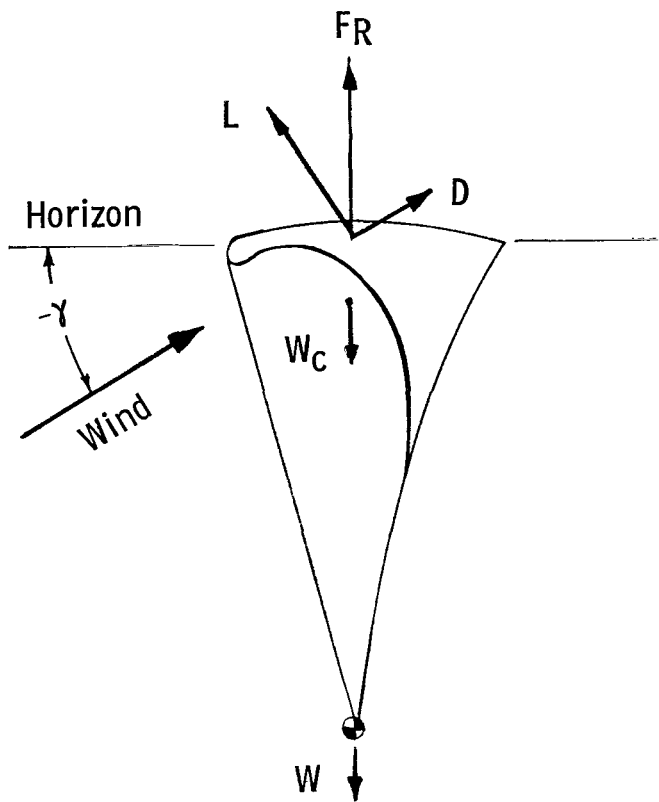
(a) Free flight.
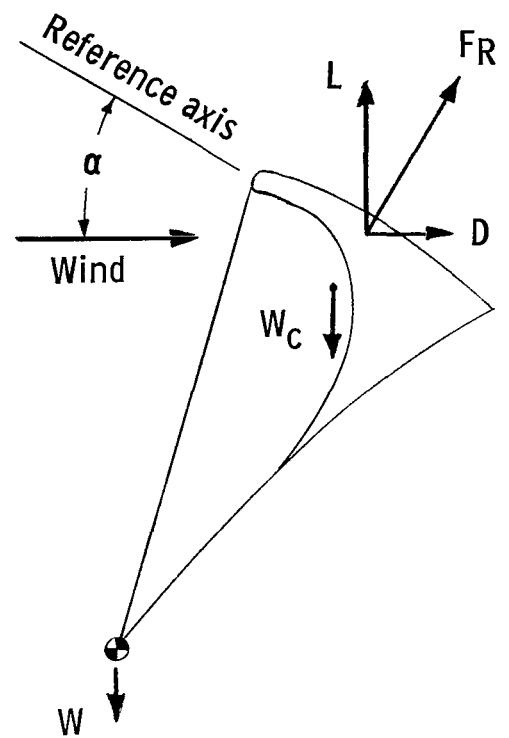
(b) Horizontal wind tunnel.
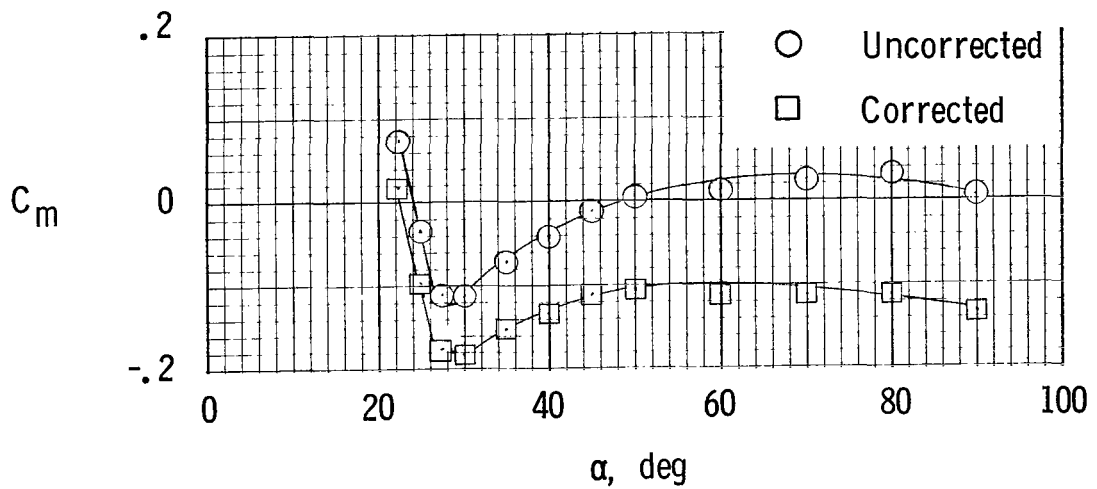
(c) Canopy-weight tare correction.

Figure 5.- Effect of weight of canopy and suspension lines on static longitudinal stability characteristics of model.

14
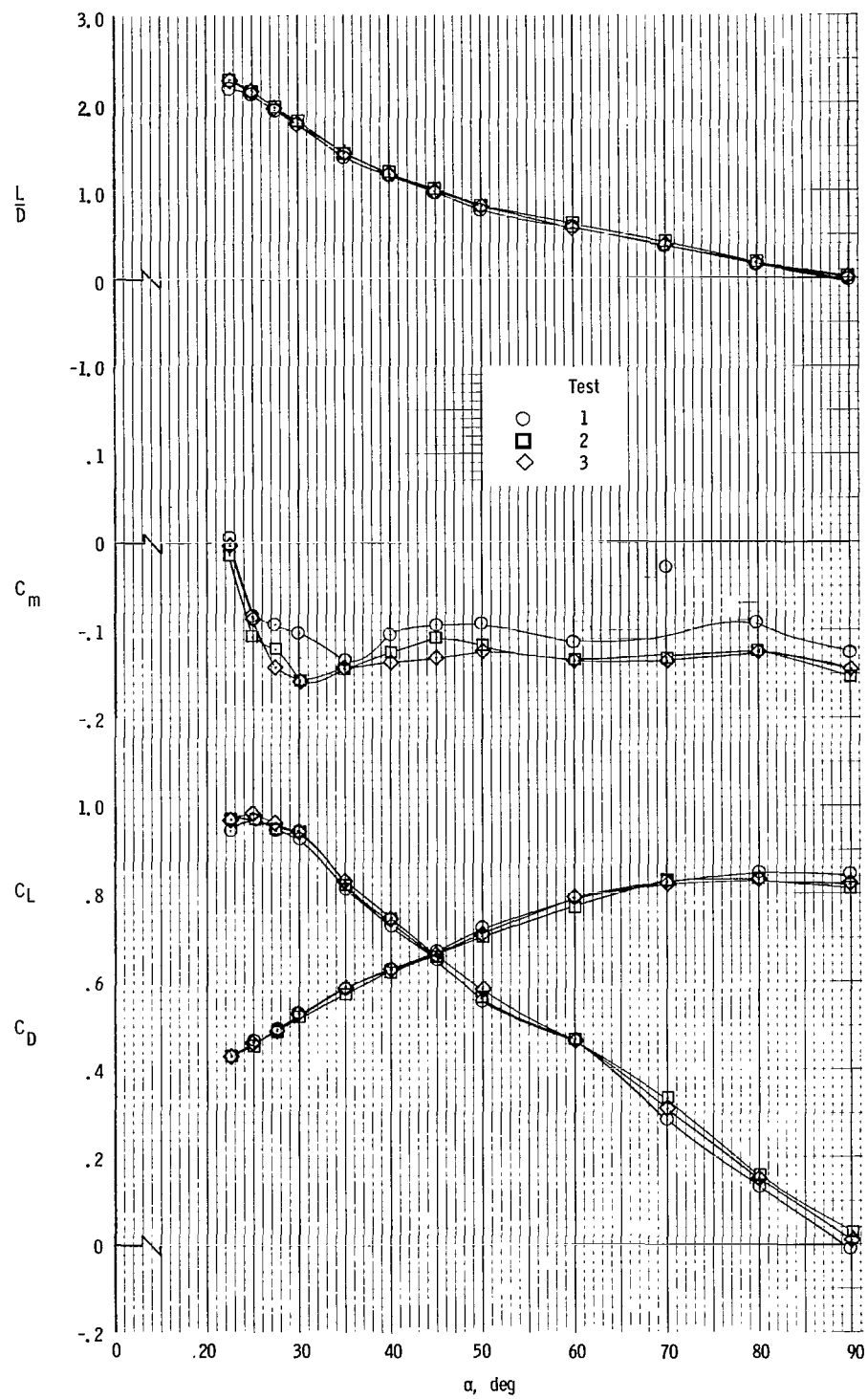
Figure 6.- Repeatability of longitudinal aerodynamic characteristics of the model. $\beta = 0^{\circ}$; $\frac{\Delta l_{L \text{ and } R}}{b} = 0.$

15
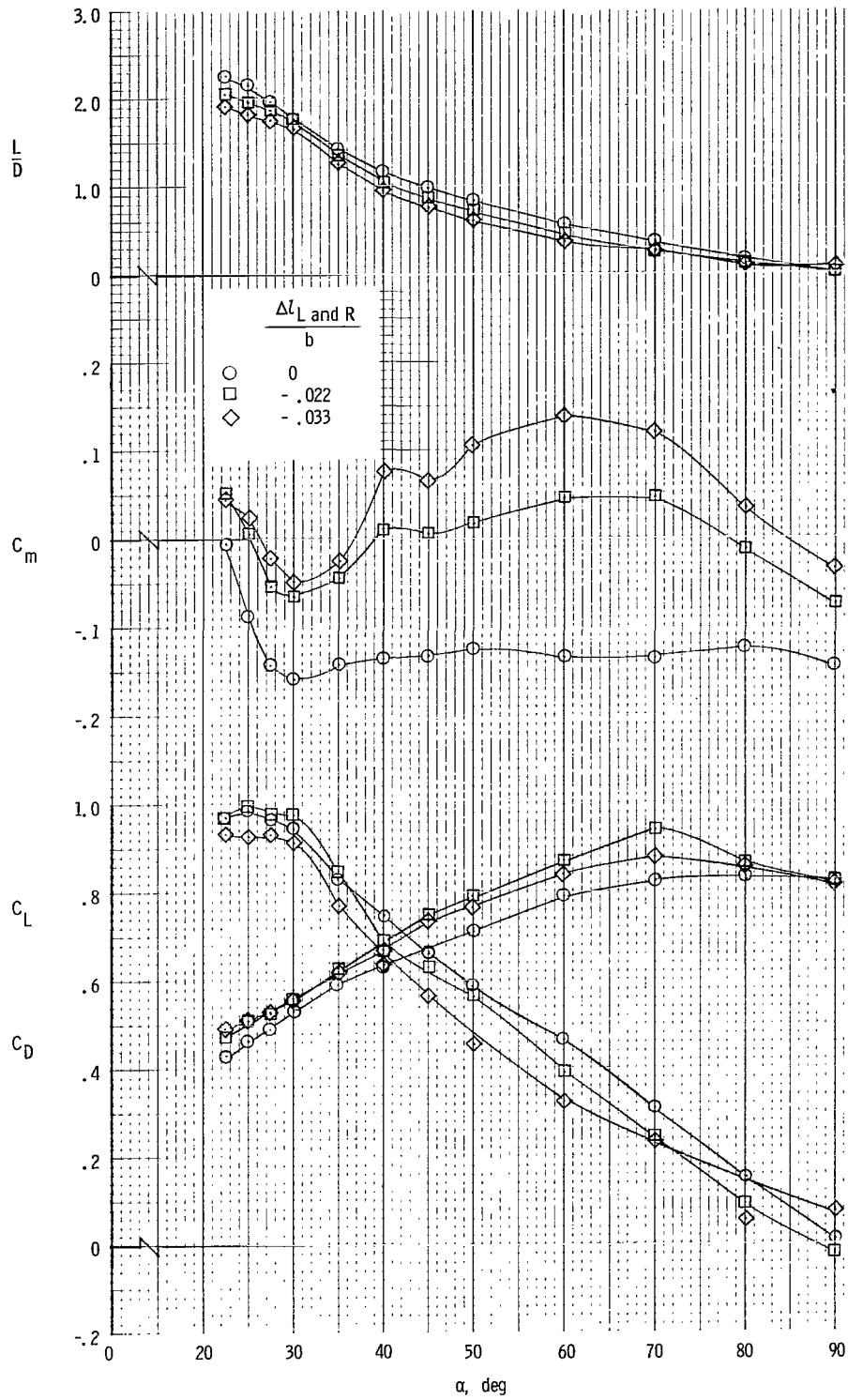
Figure 7.- Effect of changes in control-line length as a pitch control on the aerodynamic characteristics of the model. $\beta = 0^0$.
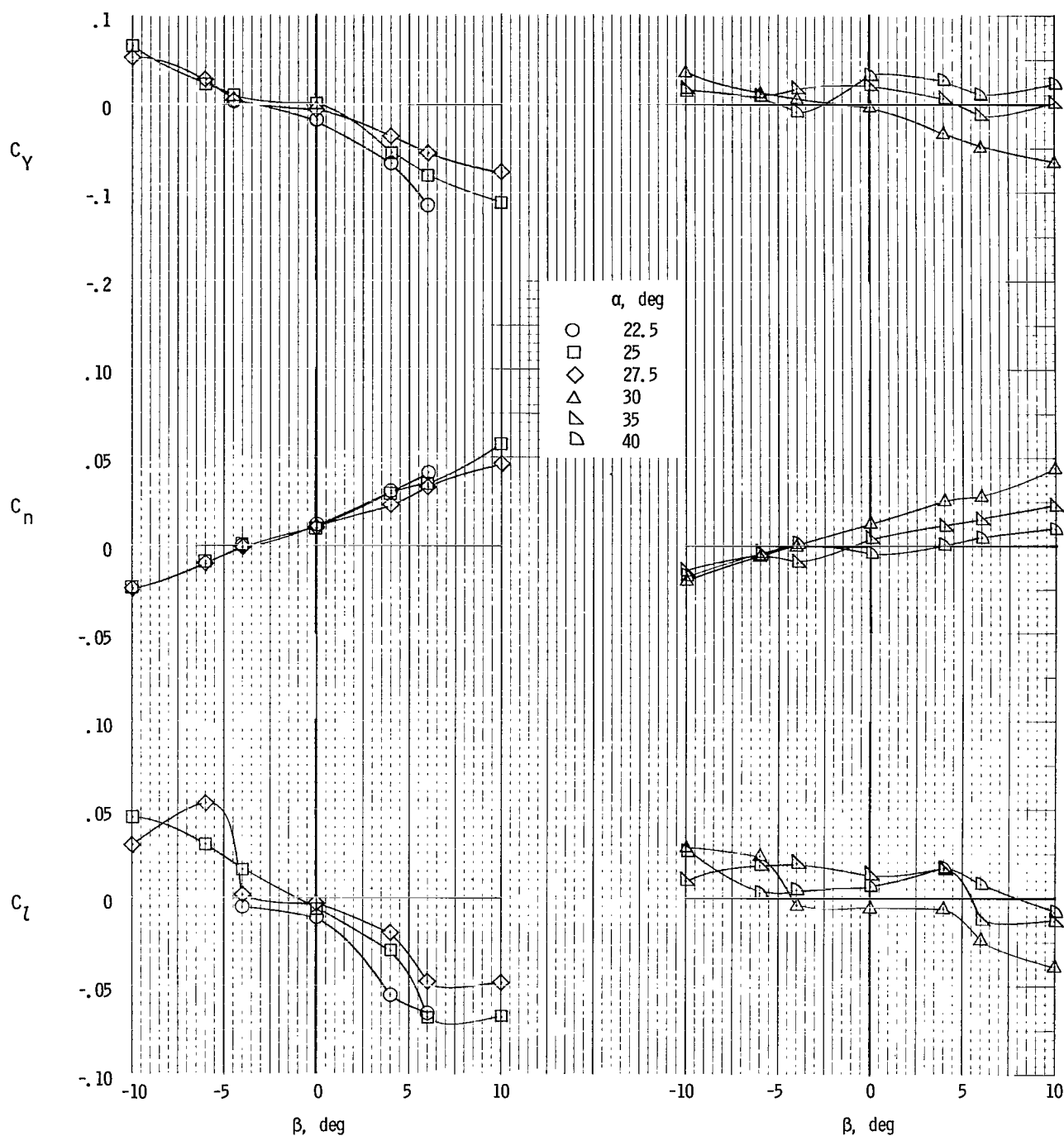
Figure 8.- Variation of lateral coefficients with angle of sideslip. $\dfrac{\Delta l_{L \text{ and } R}}{b} = 0$.
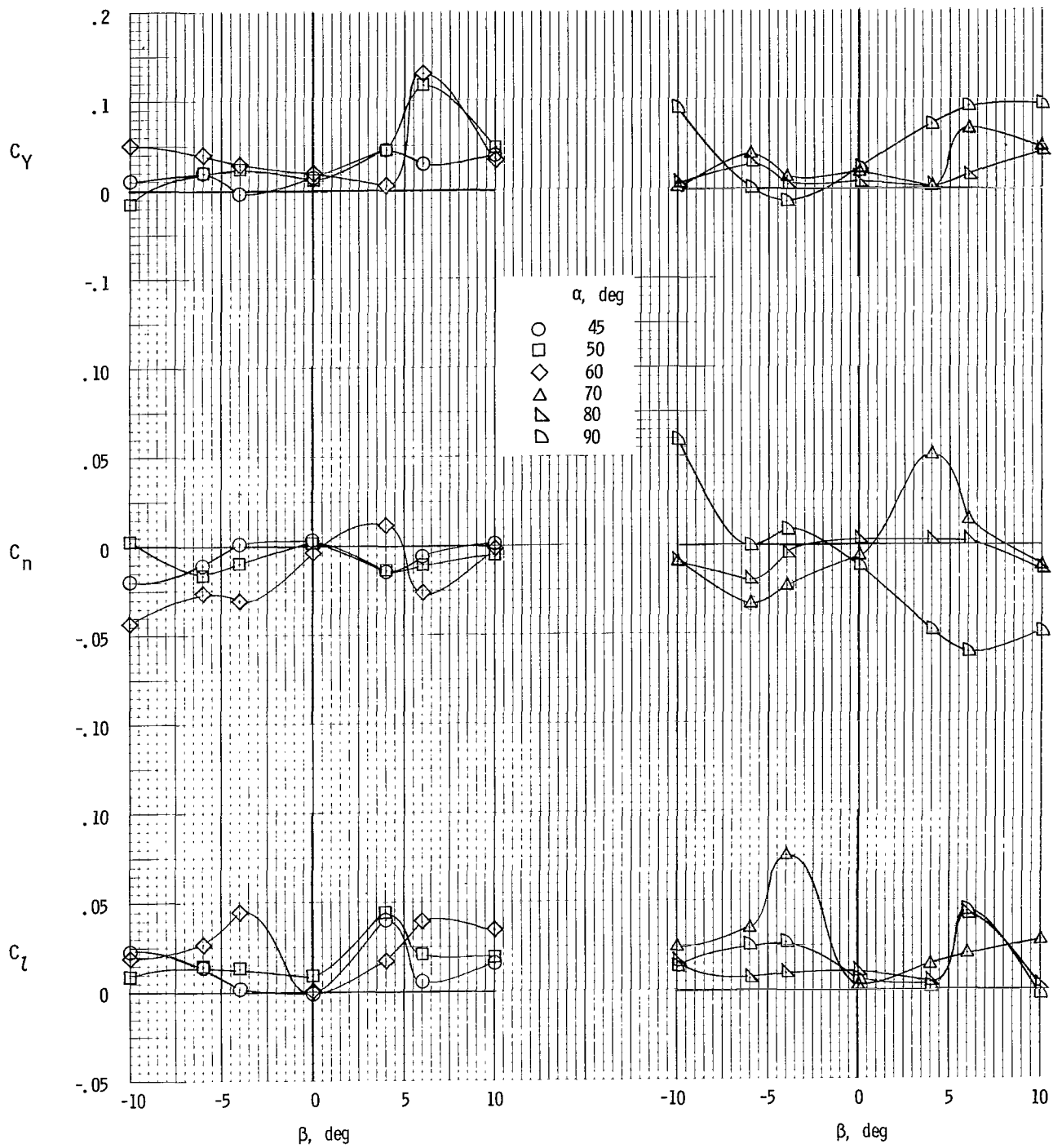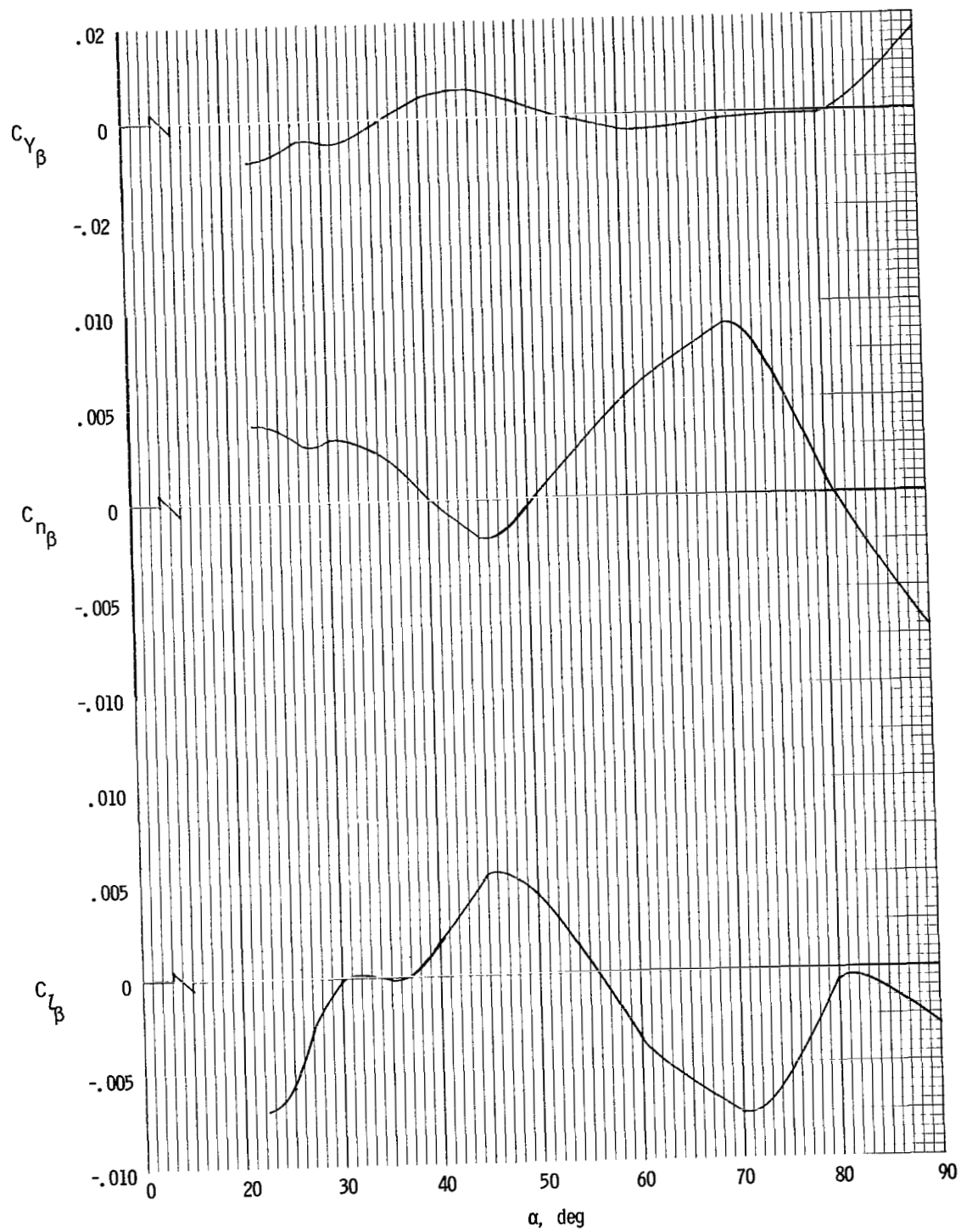
Figure 8.- Concluded.

18

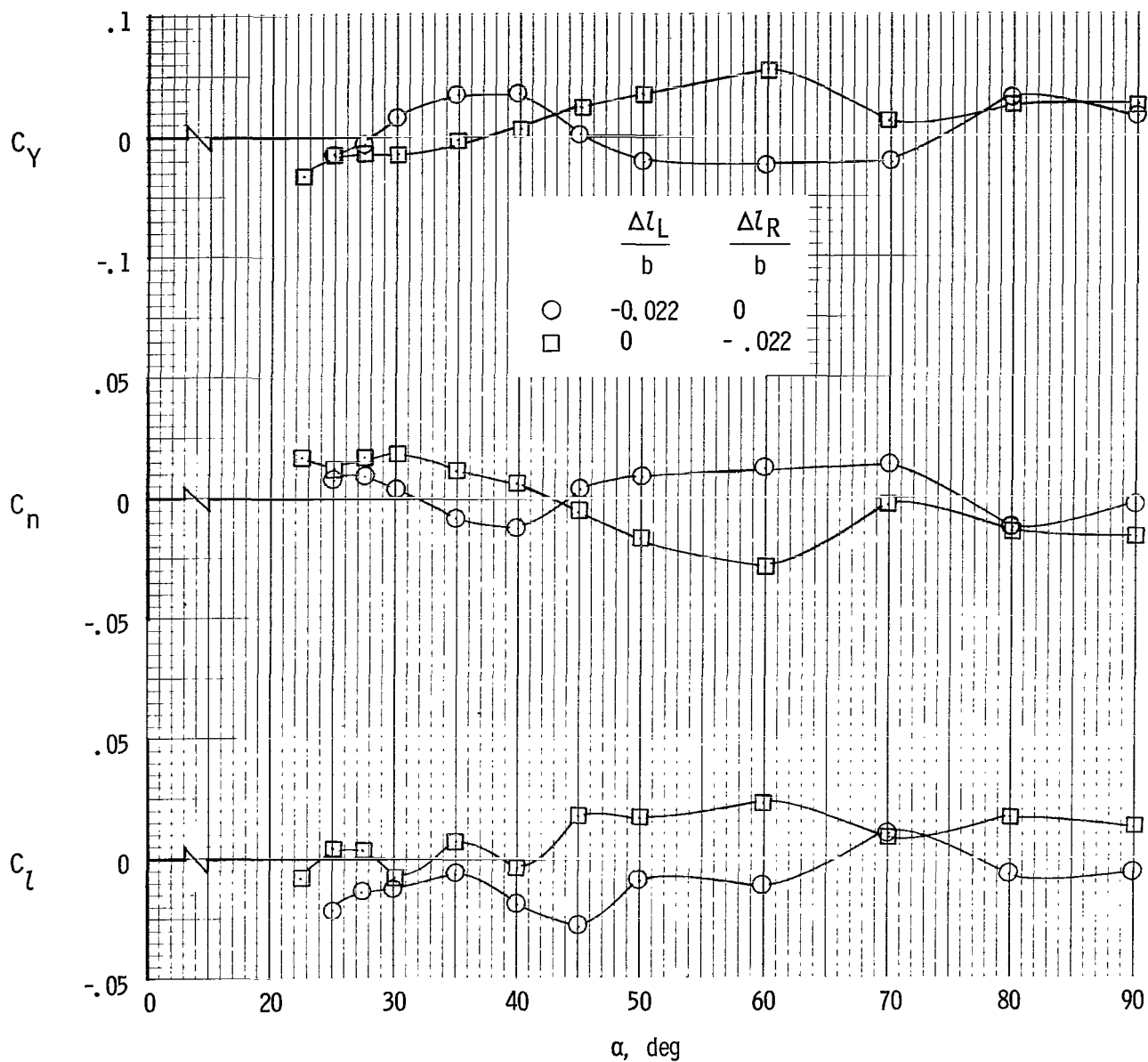Figure 9.- Lateral stability characteristics of the model. $\beta = 0^{\circ}$; $\dfrac{\Delta l_L \text{ and } R}{b} = 0$.

Figure 10.- Effect of changes in length of control lines for lateral control. $\beta = 0^0$.
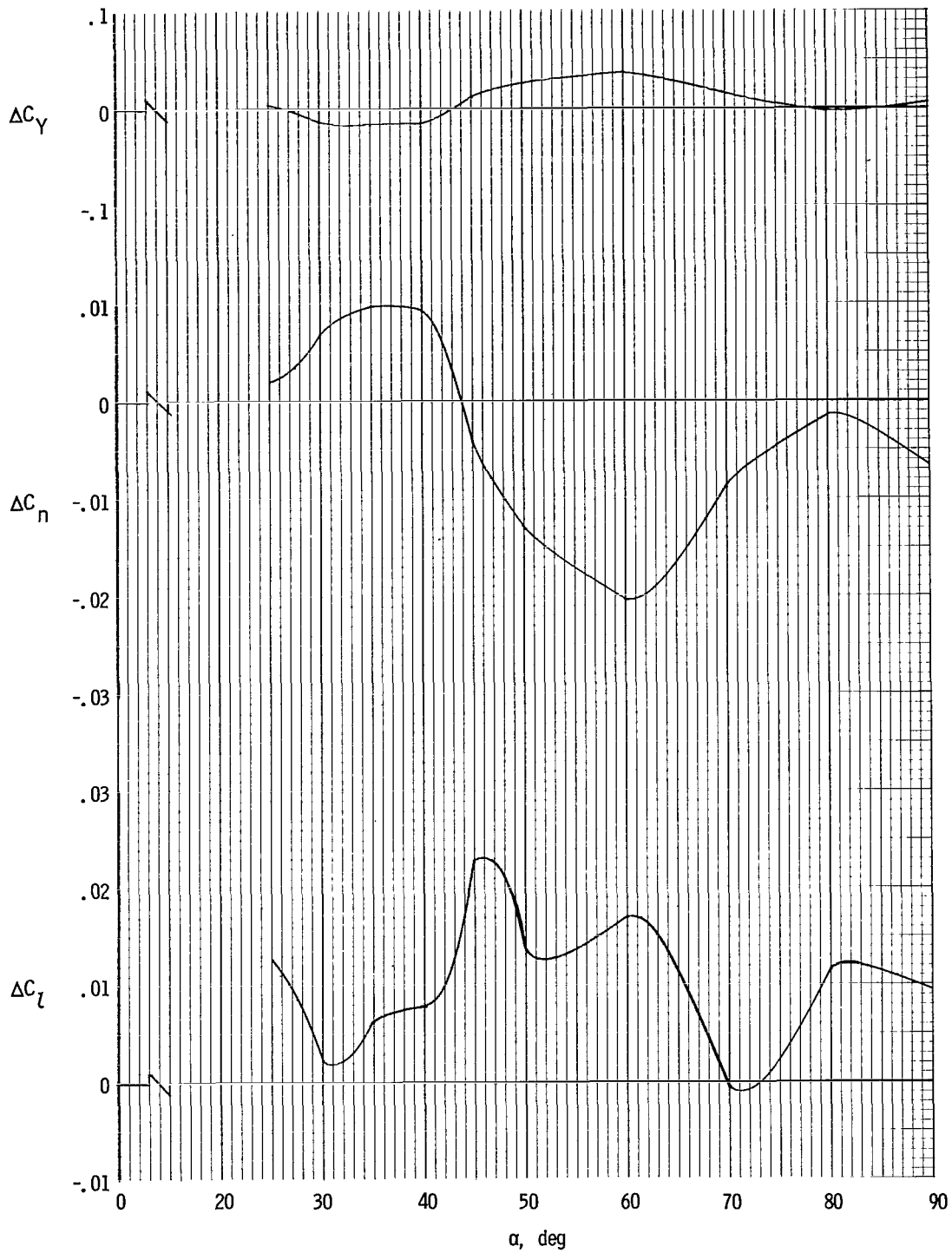
Figure 11.- Average lateral-control effectiveness. $\beta = 0°$; $\dfrac{\Delta l_L}{b} = 0$; $\dfrac{\Delta l_R}{b} = -0.022$.

"*The aeronautical and space activities of the United States shall be conducted so as to contribute . . . to the expansion of human knowledge of phenomena in the atmosphere and space. The Administration shall provide for the widest practicable and appropriate dissemination of information concerning its activities and the results thereof.*"

— NATIONAL AERONAUTICS AND SPACE ACT OF 1958

NASA SCIENTIFIC AND TECHNICAL PUBLICATIONS

TECHNICAL REPORTS: Scientific and technical information considered important, complete, and a lasting contribution to existing knowledge.

TECHNICAL NOTES: Information less broad in scope but nevertheless of importance as a contribution to existing knowledge.

TECHNICAL MEMORANDUMS: Information receiving limited distribution because of preliminary data, security classification, or other reasons.

CONTRACTOR REPORTS: Scientific and technical information generated under a NASA contract or grant and considered an important contribution to existing knowledge.

TECHNICAL TRANSLATIONS: Information published in a foreign language considered to merit NASA distribution in English.

SPECIAL PUBLICATIONS: Information derived from or of value to NASA activities. Publications include conference proceedings, monographs, data compilations, handbooks, sourcebooks, and special bibliographies.

TECHNOLOGY UTILIZATION PUBLICATIONS: Information on technology used by NASA that may be of particular interest in commercial and other non-aerospace applications. Publications include Tech Briefs, Technology Utilization Reports and Notes, and Technology Surveys.

Details on the availability of these publications may be obtained from:

SCIENTIFIC AND TECHNICAL INFORMATION DIVISION

NATIONAL AERONAUTICS AND SPACE ADMINISTRATION
Washington, D.C. 20546